

RESEARCH ARTICLE

Mutations in PIH proteins MOT48, TWI1 and PF13 define common and unique steps for preassembly of each, different ciliary dynein

Ryosuke Yamamoto¹, Shiho Yanagi¹, Masahito Nagao¹, Yuya Yamasaki¹, Yui Tanaka¹, Winfield S. Sale², Toshiki Yagi³, Takahide Kon^{1*}

1 Department of Biological Sciences, Graduate School of Science, Osaka University, Osaka, Japan, **2** Department of Cell Biology, School of Medicine, Emory University, Atlanta, Georgia, United States of America, **3** Faculty of Life and Environmental Sciences, Prefectural University of Hiroshima, Shobara, Hiroshima, Japan

* takahide.kon@bio.sci.osaka-u.ac.jp

OPEN ACCESS

Citation: Yamamoto R, Yanagi S, Nagao M, Yamasaki Y, Tanaka Y, Sale WS, et al. (2020) Mutations in PIH proteins MOT48, TWI1 and PF13 define common and unique steps for preassembly of each, different ciliary dynein. PLoS Genet 16(11): e1009126. <https://doi.org/10.1371/journal.pgen.1009126>

Editor: Susan K. Dutcher, Washington University School of Medicine, UNITED STATES

Received: March 18, 2020

Accepted: September 21, 2020

Published: November 3, 2020

Copyright: © 2020 Yamamoto et al. This is an open access article distributed under the terms of the [Creative Commons Attribution License](https://creativecommons.org/licenses/by/4.0/), which permits unrestricted use, distribution, and reproduction in any medium, provided the original author and source are credited.

Data Availability Statement: All relevant data are within the manuscript and its Supporting Information files.

Funding: This study was partially funded by grants from the Uehara Memorial Foundation (<https://www.ueharazaidan.or.jp/>), the Ito Chubei Foundation (<https://www.chubei-foundation.or.jp/>), JSPS Grant-in-Aid for Young Scientists (B) (JP17K15117) and for Scientific Research (C) (JP20K06622) (<https://www.jsps.go.jp/>) (to RY),

Abstract

Ciliary dyneins are preassembled in the cytoplasm before being transported into cilia, and a family of proteins containing the PIH1 domain, PIH proteins, are involved in the assembly process. However, the functional differences and relationships between members of this family of proteins remain largely unknown. Using *Chlamydomonas reinhardtii* as a model, we isolated and characterized two novel *Chlamydomonas* PIH preassembly mutants, *mot48-2* and *twi1-1*. A new allele of *mot48* (*ida10*), *mot48-2*, shows large defects in ciliary dynein assembly in the axoneme and altered motility. A second mutant, *twi1-1*, shows comparatively smaller defects in motility and dynein assembly. A double mutant *mot48-2; twi1-1* displays greater reduction in motility and in dynein assembly compared to each single mutant. Similarly, a double mutant *twi1-1; pf13* also shows a significantly greater defect in motility and dynein assembly than either parent mutant. Thus, MOT48 (IDA10), TWI1 and PF13 may define different steps, and have partially overlapping functions, in a pathway required for ciliary dynein preassembly. Together, our data suggest the three PIH proteins function in preassembly steps that are both common and unique for different ciliary dyneins.

Author summary

Motile cilia are hair-like organelles that protrude from many eukaryotic cells, and play vital roles in organisms including cell motility, environmental sensing and removal of infectious materials. Motile cilia are driven by gigantic motor protein complexes, called ciliary dyneins, defects in which cause abnormal ciliary motility, ultimately resulting in human diseases collectively called primary ciliary dyskinesia (PCD). Ciliary dyneins are preassembled in the cytoplasm before being transported into cilia, and preassembly requires a family of potential co-chaperones, the PIH proteins. Mutations in the PIH proteins cause defective assembly of ciliary dyneins and can result in PCD. However, despite their importance, the precise functions, and functional relationships, between the PIH proteins are unclear. In this study, using *Chlamydomonas reinhardtii*, we assessed the

National Institutes of Health Grant R01 (GM051173) (<https://www.nih.gov>) (to WSS), JSPS Grant-in-Aid for Scientific Research (C) (JP26440074) (<https://www.jsp.go.jp/>) and MEXT Grant-in-Aid for Scientific Research on Innovative Areas (JP15H01327) (<https://www.mext.go.jp/>) (to TY), and JSPS Grant-in-Aid for Scientific Research (B) (JP26291034 and JP17H03665) (<https://www.jsp.go.jp/>) (to TK). The funders had no role in the study design, data collection and analysis, decision to publish, or preparation of the manuscript.

Competing interests: The authors have declared that no competing interests exist. The funders had no role in the study design, data collection and analysis, decision to publish, or preparation of the manuscript.

functional relationship between three PIH proteins with respect to dynein preassembly and motility. We found that these PIH proteins have complicated and related roles in dynein assembly, possibly with each playing common and unique roles in dynein assembly. Our results provide new information on each conserved PIH protein for dynein assembly and provide a new understanding of PCD caused by PIH mutations.

Introduction

Motile cilia (also interchangeably referred to as flagella) are intriguing antenna-like organelles that play various important roles in eukaryotes [1, 2]. In lower eukaryotes such as *Paramecium* and *Trypanosoma*, these organelles play an indispensable role in cell motility. In higher eukaryotes including humans, cilia are essential for proper development, fertilization, and homeostasis. Defects in ciliary motility cause various symptoms including *situs inversus*, infertility, congenital heart disease and hydrocephalus in humans, collectively called as primary ciliary dyskinesia (PCD) [3, 4]. While diagnosis of PCD has attracted a good deal of attention, diagnosis can be difficult and a permanent treatment for PCD has not been established [5, 6].

The motility of cilia is driven by gigantic motor-protein complexes, referred to as ciliary dyneins that are composed of several subunits (HC: heavy chain, IC: intermediate chain, LC: light chain) and located on ciliary microtubules [1, 7–9]. Ciliary dyneins are classified into two major classes: outer dynein arm (ODA) and inner dynein arm (IDA). ODAs are particularly important for the high beat frequency of cilia, whereas IDAs are essential for creating a proper ciliary waveform [10]. Large ciliary components, including ciliary dyneins, are first assembled in the cytoplasm before being transported into and within the cilia by the intra-flagellar transport (IFT) mechanism [11–13]. This process is referred to as cytoplasmic preassembly, and many factors that are essential for the preassembly of ciliary dyneins (referred to as preassembly factors) have been reported increasing our understanding of this enigmatic process [14, 15]. Moreover, defects in the preassembly of ciliary dyneins understandably cause motility defects in cilia, resulting in PCD in humans [16–20]. In spite of its importance, the detailed mechanism of ciliary dynein preassembly in the cytoplasmic compartment, and the relationship between each preassembly factor, largely remain obscure.

In recent studies aimed at understanding of the dynein preassembly mechanism, a family of chaperone-cofactor-like proteins referred to as PIH proteins, which contain a Protein Interacting with HSP90 1 (PIH1) domain, have been shown to be tightly linked to this process [13, 17, 21] (Table 1). In vertebrates, at least four main PIH proteins (DNAAF2/KTU, PIH1D1, PIH1D2, and DNAAF6/PIH1D3) have been identified to date [13, 21, 22], and each protein has been shown to play a role in ciliary dynein preassembly [22] (Table 1), possibly residing in cytoplasmic complexes including the dynein axonemal particles (DynAPs) [23]. In *Chlamydomonas reinhardtii*, a ciliated green alga, PF13, a DNAAF2/KTU orthologue, has been shown to play an important role in the preassembly of ODAs as well as one species of IDA (IDA c) [13, 17]. Another PIH protein, MOT48 (also known as IDA10) has been shown to be necessary for the preassembly of the ODAs and a fraction of several IDA species (IDAs b, c, d, and e) [13]. In addition, a third PIH protein, TWI1 was identified in *Chlamydomonas* as an orthologue of DNAAF6/PIH1D3 [13, 21]. Among these three *Chlamydomonas* PIH proteins, knowledge of the precise function of MOT48 and TWI1 is limited, partly due to the lack of mutant alleles of the genes encoding the PIH proteins. Only the original mutant allele of *mot48*, *mot48-1* (*ida10-1*), was available for study [13]. A recent report briefly described the phenotype of a *twi1* mutant found in the CLiP library [24] as similar to wild-type [25], suggesting that there is

Table 1. PIH proteins involved in dynein preassembly.

Protein Name	Dynein Defects Caused by a Single PIH Mutation	Organism	Reference
PIH1D1	ODA, IDA “c”	<i>Danio rerio</i>	[22]
MOT48/IDA10 ^a	ODA, IDAs “b, c, d, e”, Some minor dyneins	<i>Chlamydomonas reinhardtii</i>	This study, [13, 26]
PIH1D2	ODA	<i>Danio rerio</i>	[22]
DNAAF6/PIH1D3	ODA, IDAs “f, g”	<i>Homo sapiens</i>	[18, 19, 27]
DNAAF6/PIH1D3	ODA and IDAs	<i>Mus musculus</i>	[21, 27]
PIH1D3/Twister	ODA, IDAs “c, d, g”	<i>Danio rerio</i>	[22]
TWI1 ^a	IDA “c”	<i>Chlamydomonas reinhardtii</i>	This study
DNAAF2/KTU	ODA and IDAs	<i>Homo sapiens</i>	[17, 27]
KTU	ODA and IDAs	<i>Oryzias latipes</i>	[17]
KTU	IDA “c”	<i>Danio rerio</i>	[22]
PF13 ^a	ODA, IDAs “b, c, g”, Minor dynein “DHC11”	<i>Chlamydomonas reinhardtii</i>	This study, [17, 26]

^a For dynein defects in a single *Chlamydomonas* PIH mutant, dynein species which showed > 30% reduction in spectral numbers compared to wild-type in this study were included.

<https://doi.org/10.1371/journal.pgen.1009126.t001>

no relationship between TWI1 and dynein preassembly. However, neither detailed study of ciliary dynein assembly nor an examination of the relationship of TWI1 to the other PIH proteins has been performed.

In this study, we report the isolation/characterization of a *twi1-1* mutant and a new allele of the *mot48*, *mot48-2*. The *mot48-2* mutants swim more slowly than wild-type and have a large defect in assembly of dyneins in the ciliary axoneme. The *twi1-1* mutant has only a slightly reduced motility, as previously described [25], and has only a slight defect in dynein assembly in the axoneme. In addition, a double mutant *mot48-2; twi1-1* are more severely defective in motility and dynein assembly than either of the parent PIH mutant strains. Similarly, the double mutant *pf13; twi1-1* also shows a more severe phenotype than the parent, single mutants. These results strongly suggest that PIH proteins MOT48, TWI1 and PF13 define different steps, and have partially overlapping functions, in a pathway required for ciliary dynein preassembly.

Results

Isolation and characterization of *mot48-2*, a novel allele of *mot48* (*ida10*)

We identified a slow swimming strain (LMJ.RY0402.055540) in the *Chlamydomonas* mutant library (CLiP) [24], with a swimming pattern that was reminiscent of the *mot48-1* mutant previously described [13]. The strain carried an additional mutation other than the original *APH-VIII* insertion used to establish the library [24]. After back-crossed to wild type (CC-125) cells, we determined the MOT48 protein [13, 28] is indeed missing from mutant progeny from the cross (Fig 1A). We examined the *MOT48* sequence in the mutant progeny, and found a mutation (G>T) in the fourth exon, which results in a pre-mature stop codon. Thus, we named the new mutant allele *mot48-2* (Fig 1B) [13]. Immunoblots of whole cell samples from *mot48-1* and *mot48-2* show no evidence of MOT48 (Fig 1A) [13]. The mutation in *mot48-2* is predicted to disrupt the PIH1 domain in MOT48, deleting the potential binding motif for chaperones including HSP90 (Fig 1C) [13, 17, 29, 30]. As has been noted for *mot48-1* [13], the *mot48-2* mutants typically swim much slower ($\sim 85 \pm 14 \mu\text{m/s}$) than wild-type (CC-125 = $\sim 136 \pm 21 \mu\text{m/s}$), although the motility varies slightly from day to day and culture to culture. A transgene expressing the wild-type MOT48 with a 3HA tag at the C-terminus (*mot48-2; MOT48::HA*) rescued swimming velocity ($\sim 131 \pm 31 \mu\text{m/s}$) and expression of the 3HA-tagged

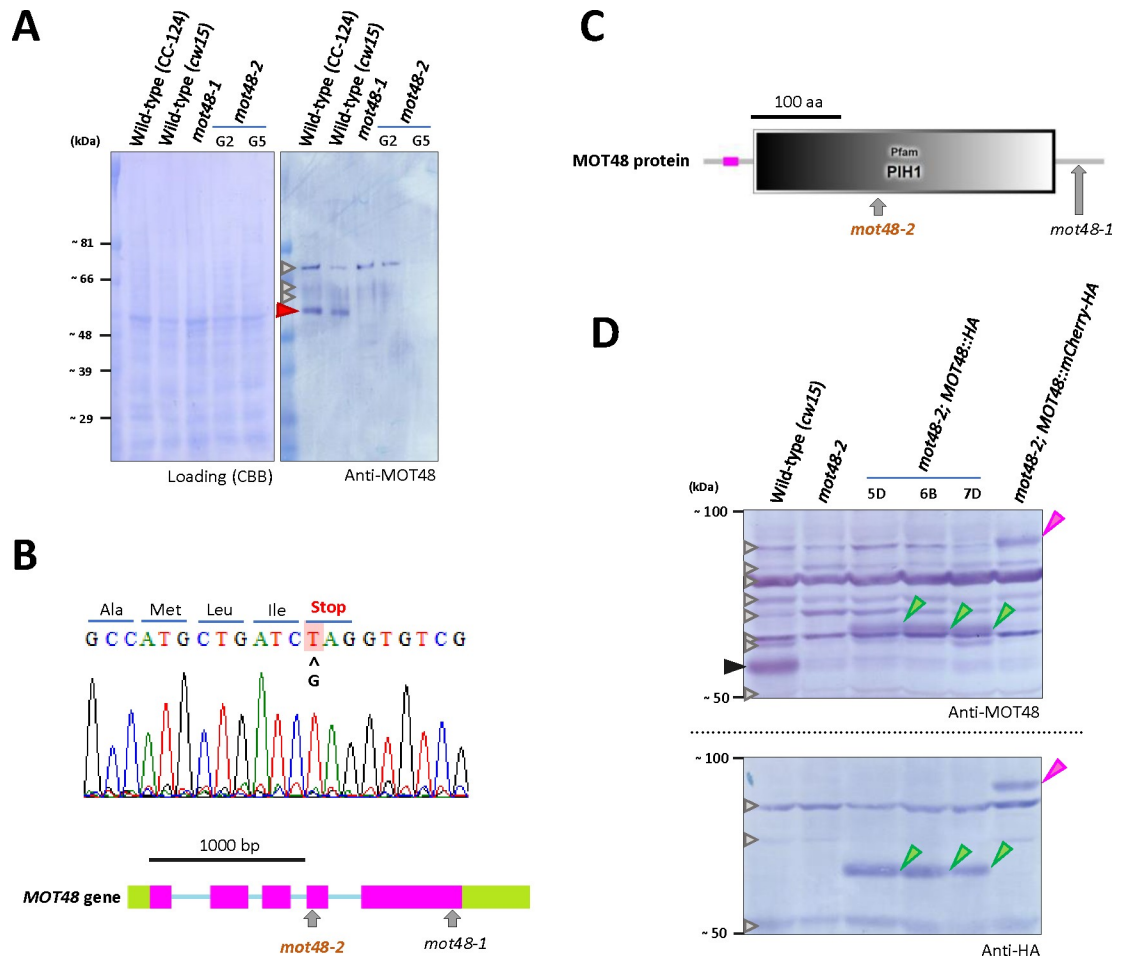


Fig 1. Characterization of a novel *mot48* allele, *mot48-2*. A) Immunoblotting analysis of whole cell samples from wild-type (CC-124, *cw15*), *mot48-1*, and two clones of *mot48-2* (G2/G5) using an anti-MOT48 antibody. The MOT48 protein band (red arrowhead) is missing in all *mot48* strains, although we cannot completely rule out the possibility that tiny amounts of MOT48 are expressed in an altered form in *mot48-1*. Gray arrowheads: non-specific bands. B) Sequence analysis of the *mot48-2* genomic DNA identified a point mutation (G>T) in the fourth exon of MOT48, resulting in a premature stop codon. The *MOT48* genomic structure is based on/from Phytozome (v5.5: https://phytozome.jgi.doe.gov/pz/portal.html#!info?alias=Org_Creinhartii) and JGI (v4: <https://genome.jgi.doe.gov/Chlre4/Chlre4.home.html>) *Chlamydomonas* genome databases (Pink: Exon, Blue: Intron, Green: UTR). The mutation sites in *mot48-1* and *mot48-2* are indicated. C) The molecular structure of the MOT48 protein was predicted using a SMART analysis (<http://smart.embl-heidelberg.de/>). MOT48 has a PIH1 domain in the middle of its structure (gray). The pink bar represents a low-complexity region. The *mot48-1* mutant has a mutation near the C-terminus of the MOT48 molecule [13], while the new allele (*mot48-2*) has a mutation in the middle of the molecule. D) Immunoblot analyses of whole cell samples of wild-type (*cw15*), *mot48-2*, three independent colonies of *mot48-2*; *MOT48::HA* (5D, 6B, 7D) and one colony of *mot48-2*; *MOT48::mCherry-HA* using the anti-MOT48 and anti-HA antibodies. The MOT48 protein band (black arrowhead) present in the wild-type strain is absent in *mot48-2*. In the *mot48-2*; *MOT48::HA* strain, exogenous MOT48 with a 3HA tag is expressed in all three independent colonies (green arrowheads). In the *mot48-2*; *MOT48::mCherry-HA*, exogenous MOT48 with a large mCherry-3HA tag is expressed (pink arrowhead), partially rescuing the Mot48 (Ida10) phenotype. Gray arrowheads: non-specific bands.

<https://doi.org/10.1371/journal.pgen.1009126.g001>

MOT48 (Fig 1D). The Mot48 phenotype was also rescued by a transgene expressing MOT48 with an added C-terminal mCherry-3HA tag (*mot48-2*; *MOT48::mCherry-HA*) (swimming velocity = $\sim 120 \pm 21 \mu\text{m/s}$) (Fig 1D and S1 Fig).

Since MOT48 has previously been reported to function in ciliary dynein preassembly and *mot48-1* cilia lacked a subset of dynein species [13], we assessed ciliary dynein assembly in the *mot48-2* mutants. To semi-quantitatively estimate the amount of each dynein species in the

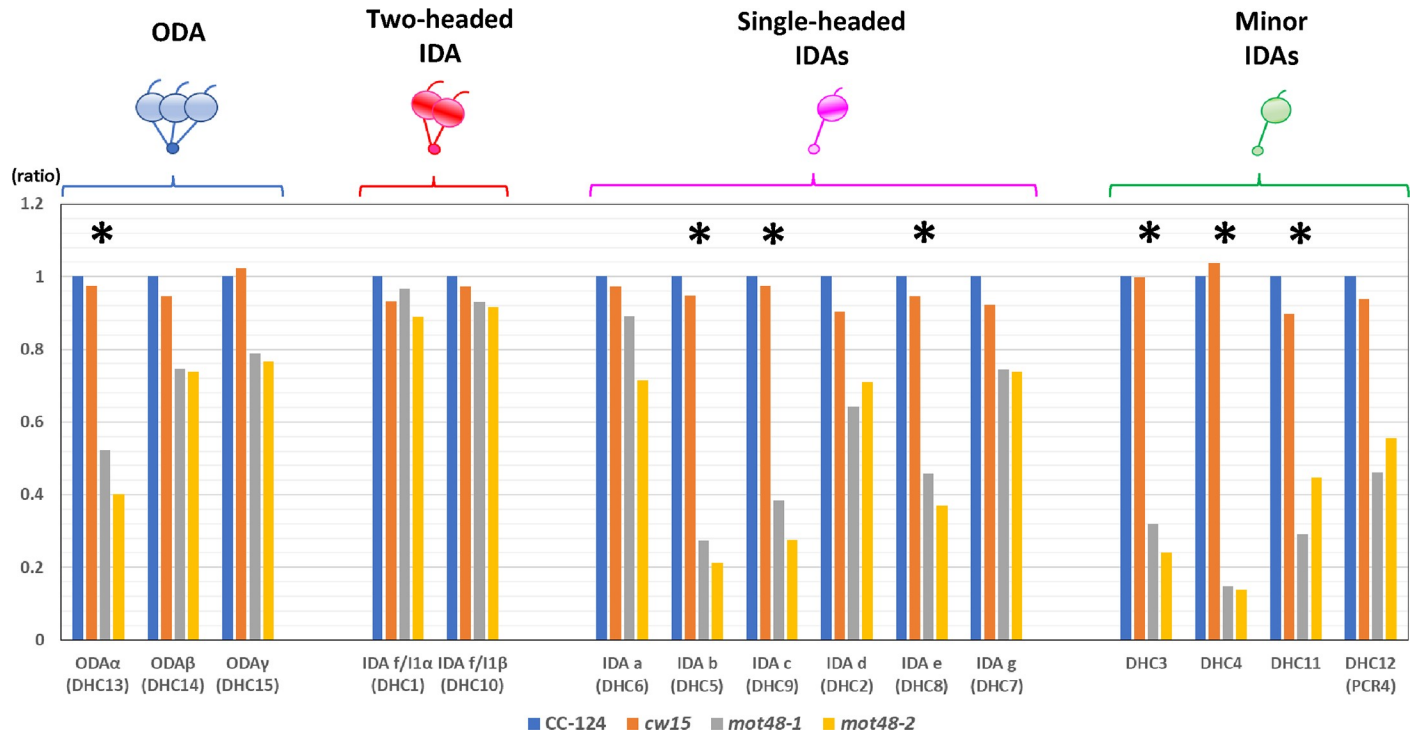


Fig 2. Several IDAs are deficient in the *mot48-2* ciliary axonemes. Spectral counting results (first set) of ciliary axonemal dyneins in wild-type (CC-124 and *cw15*), *mot48-1*, and *mot48-2* strains. The spectral numbers observed in the mutants were normalized using spectral numbers observed in the CC-124 wild-type strain. Asterisks indicate the ciliary axonemal dynein species for which the spectral numbers in *mot48-2* were below 50% of the levels in the CC-124 strain.

<https://doi.org/10.1371/journal.pgen.1009126.g002>

mot48-2 cilia compared to wild-type (CC-124), spectral counting experiments were performed on isolated axonemes (Fig 2). Among the 15 species of ciliary dynein HCs present in the *Chlamydomonas* genome [8, 26], ODA α , IDAs b (DHC5), c (DHC9), and e (DHC8), and three minor dyneins DHC3, DHC4, and DHC11 levels are greatly reduced compared to wild-type axonemes (< 50%). In addition, ODAs β and γ , IDAs a (DHC6), d (DHC2), and g (DHC7), and one minor dynein (DHC12/PCR4 [26, 31]) show a more modest reduction in the *mot48-2* mutants (50% ~ 80% of the levels of wild type) (Relationship of dynein subunits in *Chlamydomonas* and humans is summarized in S1 Table). Immunofluorescent microscopic observation also confirmed the defects of IDA c (DHC9) and DHC11 (a minor species) in the *mot48-2* axonemes (S2 Fig). The HCs of the two-headed IDA f/I1 showed only a slight reduction in *mot48-2* mutants (Fig 2).

Characterization of the *twi1-1* mutant, which lacks a PIH protein required for dynein preassembly

In addition to MOT48, two other PIH proteins have been identified in *Chlamydomonas* [13]. One is PF13, a protein required for ciliary dynein assembly based on characterization of the dynein-deficient mutant *pf13* [32]. Defects of its orthologue in mammals (DNAAF2/KTU) have been reported to cause the ciliopathy [17] (Table 1). The other is the TWI1 protein (Fig 3A) (predicted molecular weight = ~ 20590), and defects in the TWI1 orthologue (DNAAF6/PIH1D3) also cause the ciliopathy [18, 19, 21] (Table 1). In addition, the expression of TWI1 is highly induced upon deciliation [33]. A *twi1* strain (LMJ.RY0402.076787) was recently identified in the CliP library [24], and reported that the swimming phenotype of this LMJ.RY0402.076787 strain is similar to wild-type [25]. Thus, we back-crossed the LMJ.

RY0402.076787 strain to wild-type (CC-125) and the *twi1* progeny (*twi1-1*) phenotype was characterized. Compared to wild-type *Chlamydomonas* (CC-125) ($\sim 136 \pm 21 \mu\text{m/s}$), the *twi1-1* swims at a slightly reduced rate ($\sim 103 \pm 14 \mu\text{m/s}$) after the 3-day liquid culture, suggesting *twi1-1* had subtle defects in assembly of ciliary dyneins (S1 Fig). Like other mutants defective in genes encoding PIH proteins, the swimming phenotypes vary slightly from day to day.

An antibody against TWI1 was generated, and we noticed that TWI1 shows two or three bands on immunoblots (Fig 3B–3D). Since these TWI1 bands could be observed even in freshly-boiled *Chlamydomonas* whole cell SDS-PAGE samples, we presume that these band shifts represent modified forms of TWI1, rather than protein degradation. We assessed if the TWI1 band patterns were altered following treatment with calf intestinal phosphatase, and found that no changes occurred, suggesting these shifts did not arise as a result of TWI1 phosphorylation. Also, we could not identify alternative-splicing variants of *TWI1* cDNA. One possibility is that the TWI1 protein is structurally stable, and that boiling/SDS-treatment is not sufficient to completely denature the protein, as has been observed for another preassembly factor CCDC103 [34].

To test if the IFT-related or preassembly-related mutations affect the stability of the TWI1 proteins, we performed the immunoblots using the TWI1 antibody on the whole cell samples from various IFT-related and preassembly-related mutants. Immunoblots reveal the TWI1 protein is present in most IFT-related and preassembly-related mutants (e.g. *ift46-1*, *ift74-1*, and *oda5*) (Fig 3B) (See S1 Table summarizing *Chlamydomonas* and human proteins). Surprisingly, *pf22* (CC-1382) and *pf23* (CC-1383 and CC-3660) strains completely lack TWI1 (Fig 3B–3D). In contrast, immunoblots of whole cell samples from *pf22* (CC-2495), *pf22A* (CC-2493), and *pf23* (5–4) strains have normal levels of TWI1 (Fig 3C and 3D). The result strongly suggested TWI1 loss in *pf22* (CC-1382) and *pf23* (CC-1383 and CC-3660) strains occurs because of an additional mutation. *TWI1* sequence in these mutant strains revealed the transposon MRC1 ($\sim 1,600$ bp) [35] inserted in the fourth intron of the *TWI1* gene (Fig 3A). Since these strains were first isolated in Dr. David Luck's laboratory in the 1970's [32], we suspect that some of the parent strains used for mutagenesis in Luck laboratory had this transposon insertion in *TWI1* gene, and that these strains (*pf22* (CC-1382) and *pf23* (CC-1383 and CC-3660)) are actually double mutants lacking their respective proteins (*Chlamydomonas* PF22 or PF23) and TWI1. Other *pf* strains from Luck laboratory might also carry this *twi1* (*twi1-2*) background. We carried out spectral counting experiments (Fig 4) of the ciliary axonemal dyneins in the *twi1-1* mutant, and found that only the levels of IDAs c (DHC9) and e (DHC8) were modestly reduced compared to wild-type (CC-125). This observation is consistent with the mild motility phenotype of *twi1-1*.

***Chlamydomonas* PIH proteins MOT48, TWI1, and PF13 have overlapping and unique roles in assembly of different ciliary dyneins**

We took advantage of *Chlamydomonas* genetics by isolating double PIH mutants (*mot48-2*; *pf13*, *mot48-2*; *twi1-1* and *pf13*; *twi1-1*) from crosses between single PIH mutants (*pf13*, *mot48-2*, and *twi1-1*). The predictions included that if deleted proteins function together in the same path and a phenotype of one mutant is similar or the same as the other, then the double mutant phenotype would nearly match the phenotype of the single mutants. Also, if deleted proteins function together in the same path but a phenotype of one mutant is more severe to the other, then the double mutant phenotype would match the phenotype of the more deleterious single mutant. Alternatively, if the deleted proteins operate in different pathways, or have some overlapping function but do not function together in the same path, then the double mutants would have a more severe phenotype than the single mutants.

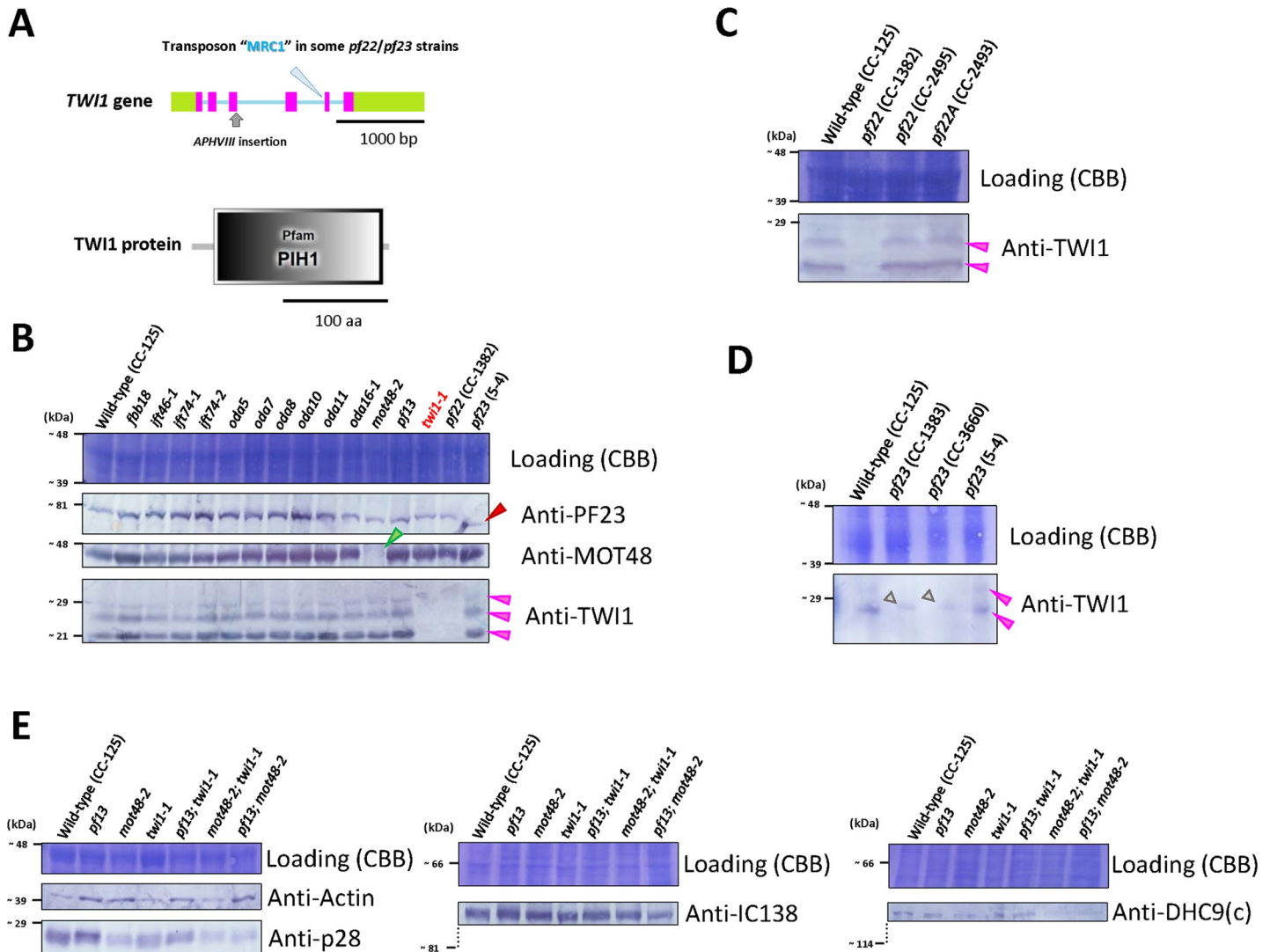


Fig 3. TWI1 is a dynein preassembly factor present in various ciliary mutants. A) Genomic structure of *Chlamydomonas* TWI1 gene based on/from the Phytozome (v5.5: https://phytozome.jgi.doe.gov/pz/portal.html#info?alias=Org_Creihardtii) and JGI (v4: <https://genome.jgi.doe.gov/Chlre4/Chlre4.home.html>) genome databases (Pink: Exon, Blue: Intron, Green: UTR). The insertional mutation site in the *twi1-1* mutant is based on previous reports [24, 25]. The insertion site of the transposon, MRC1, in some of the *pf22/pf23* strains determined in this study is shown with a light blue arrowhead. The molecular structure of the TWI1 protein predicted by SMART analysis (<http://smart.embl-heidelberg.de/>) is also shown. TWI1 has a PIH1 domain in the middle of its structure (gray). B) Immunoblot of whole cell samples from various IFT-related and dynein preassembly mutants using anti-PF23, MOT48, and TWI1 antibodies. All mutants, except for *twi1-1* and *pf22* (CC-1382) show the presence of TWI1 in whole cells. As discussed in the text, TWI1 protein was visualized as consisting of two or three bands on immunoblots (pink arrowheads). The *pf23* (5-4) strain had a slightly smaller and mutated PF23 protein, as described previously (red arrowhead) [28]. The *mot48-2* mutant lacked the MOT48 protein (green arrowhead). C) Immunoblotting of whole cell samples from wild-type (CC-125) and three *pf22* strains (*pf22* (CC-1382), *pf22* (CC-2495), and *pf22A* (CC-2493)) using an anti-TWI1 antibody. *pf22* (CC-1382) lacked the TWI1 protein (pink arrowheads) in whole cells, because of the insertion of the *Chlamydomonas* transposon, MRC1, in the fourth intron (see A in this figure). D) Immunoblotting of whole cell samples from wild-type (CC-125) and three *pf23* strains (*pf23* (CC-1383), *pf23* (CC-3660), and *pf23* (5-4)) using the anti-TWI1 antibody. *pf23* (CC-1383) and *pf23* (CC-3660) lacked the TWI1 protein (pink arrowheads) in whole cells, because of insertion of the transposon, MRC1. *pf23* (5-4) had a normal TWI1 protein. Gray arrowheads: non-specific bands. E) Immunoblottings of the de-ciliated cell body samples from wild-type (CC-125) and single or double PIH mutants using the antibodies against various IDA subunits (p28/IDA4, actin/IDA5, IC138/BOP5, and DHC9/IDA c HC).

<https://doi.org/10.1371/journal.pgen.1009126.g003>

The motility phenotype of the *mot48-2; twi1-1* double mutant is worse than the *mot48-2* single mutant (swimming velocity: *mot48-2* = $\sim 85 \pm 14 \mu\text{m/s}$; *mot48-2; twi1-1* = $\sim 49 \pm 13 \mu\text{m/s}$). Furthermore, about half of the double mutant cells have completely non-motile cilia while the other half of the cells display a slow swimming phenotype (S1 Fig). In addition, the

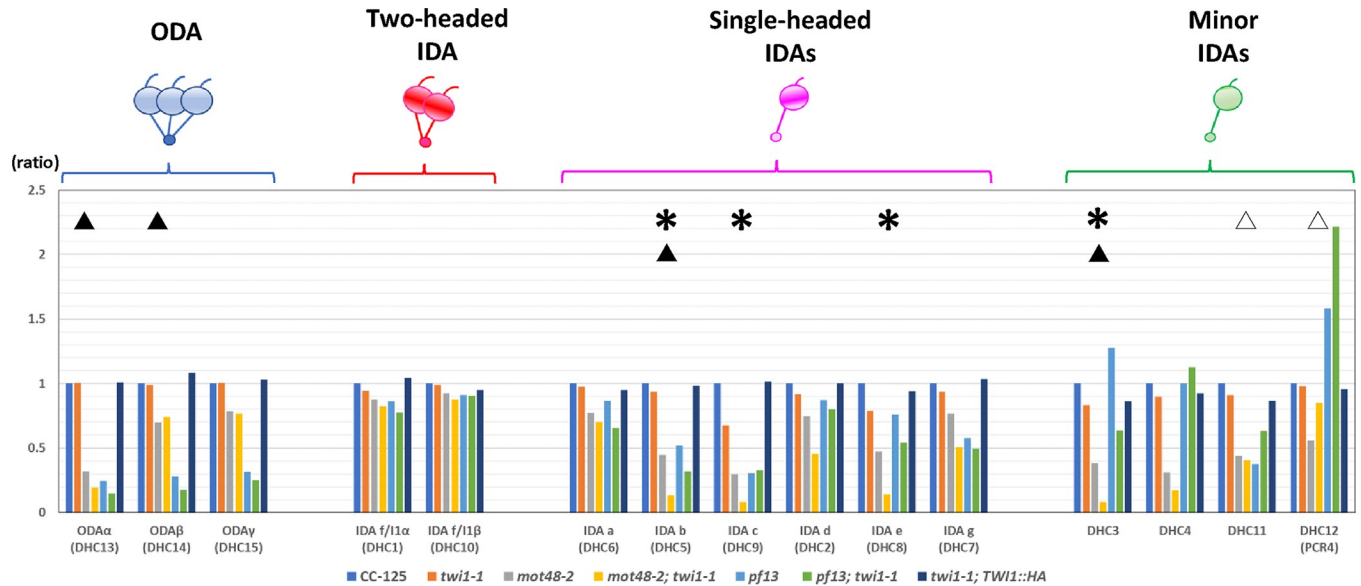


Fig 4. Dynein defects are profound in double PIH preassembly mutants. Spectral counting results (second and third sets combined) of ciliary axonemal dyneins from wild-type (CC-125), *twi1-1*, *mot48-2*, *mot48-2; twi1-1*, *pf13*, *pf13; twi1-1* and *twi1-1; TWI1::HA*. The spectral numbers observed in the mutants were normalized using the spectral numbers from the CC-125 strain. Asterisks indicate the ciliary dynein species for which the spectral numbers in the *mot48-2; twi1-1* strain showed more than a 50% reduction compared to the *mot48-2* strain. The black triangles indicate the ciliary dynein species for which the spectral numbers in the *pf13; twi1-1* strain showed a more than 30% reduction compared to the *pf13* strain. DHC11 and DHC12 showed ~ 50% increase in *pf13; twi1-1* compared to *pf13* (white triangles).

<https://doi.org/10.1371/journal.pgen.1009126.g004>

percentage of ciliated cells of the *pf13; twi1-1* double mutant (~ 16%) is much lower than the *pf13* (~ 58%) single mutant. These observations strongly suggest that TWI1 protein is involved in ciliary dynein preassembly.

To further test the idea that dynein assembly is more defective in the double mutants, we performed spectral counting experiments on dyneins in isolated axonemes from the double and single PIH preassembly mutants to compare the amount of ciliary dyneins assembled (Fig 4). The *mot48-2; pf13* double mutant grew extremely short cilia or was missing cilia. This severe phenotype hindered comparison of the amount of ciliary dynein assembled in this strain. This short cilia phenotype was also previously observed in the *mot48-1; pf13* mutant [13]. Predictably, this short-cilia phenomenon was a consequence of pre-assembly failure of sufficient number of ciliary dyneins required for ciliary elongation.

The peptide numbers for a subset of ciliary dyneins in the *mot48-2; twi1-1* double mutant are greatly reduced compared to *mot48-2* (Fig 4). In particular, the IDAs b (DHC5), c (DHC9), and e (DHC8), and one minor dynein, DHC3 are greatly reduced in the double mutant compared to *mot48-2* alone. This result indicates that both MOT48 and TWI1 function in the preassembly of these dynein species, but in possibly different steps. Alternatively, MOT48 and TWI1 have overlapping functions in the same step of preassembly, and loss of the two PIH proteins cause severe defects for some ciliary dyneins. Peptide numbers of ODAs α and β , and IDA b (DHC5) in the *pf13; twi1-1* double mutant are modestly reduced compared to the *pf13* mutant, indicating that PF13 and TWI1 both function in the preassembly of these dyneins possibly in different steps, and/or have some overlapping function in the same step (see Discussion).

It is intriguing that peptide numbers of some minor dyneins (DHC12 in the *mot48-2; twi1-1* double mutant, and DHC11 and DHC12 in the *pf13; twi1-1* double mutant) are much greater in the double PIH mutants than in the single PIH mutants (*pf13*, *mot48-2*, and *twi1-1*) (Fig 4).

This result suggests that the preassembly of these minor dynein species is not affected by the double PIH mutations and that these minor dyneins partially replace the major dynein species that are affected in these double mutants. While some major IDAs are predicted to be replaced by minor dynein species at the proximal end of the cilia [36, 37], replacement of major dynein species by minor dynein species, especially DHC12 in the double PIH mutants, must be confirmed by future biochemical studies.

In addition, to check the stability of various dynein subunits in the cytoplasm, we performed immunoblots of de-ciliated cell-body samples. Immunoblots of dynein subunits (S1 Table) on the de-ciliated cell-body samples of the single or double PIH mutants revealed that one IDA subunit, p28/IDA4 was apparently reduced in the cell bodies from PIH mutants with *mot48* background (Fig 3E). In contrast, another IDA subunit, actin/IDA5 appeared to accumulate in the cell bodies from PIH mutants with the *pf13* and/or *mot48* background (Fig 3E). The reduction in p28/IDA4 and increase in actin/IDA5 were also previously observed in *mot48-1* [13]. In addition, IDA c HC (DHC9) is reduced in the PIH mutants with the *mot48* background (Fig 3E).

As a further test, we performed rescue experiments to see if recovery of the TWI1 protein in the *twi1-1* and *mot48-2*; *twi1-1* would rescue the observed phenotypes. Exogenously expressed TWI1::3HA proteins in *twi1-1*; TWI1::HA and *mot48-2*; *twi1-1*; TWI1::HA (S2 Table) successfully rescue both the swimming defects (swimming velocity: *twi1-1* = $\sim 103 \pm 14 \mu\text{m/s}$; *twi1-1*; TWI1::HA = $\sim 121 \pm 21 \mu\text{m/s}$; *mot48-2*; *twi1-1* = $\sim 49 \pm 13 \mu\text{m/s}$; *mot48-2*; *twi1-1*; TWI1::HA = $\sim 71 \pm 11 \mu\text{m/s}$) and ciliary dynein assembly (Figs 4 and 5A–5C and S1 Fig). Notably, the expressed exogenous TWI1::3HA proteins by the cDNA rescue show several forms in the immunoblots (Fig 5A), suggesting these variants most likely derive from structural differences or some modification rather than alternative splicing or protein degradation. These results indicate that the observed phenotypes in *twi1-1* and *mot48-2*; *twi1-1* were indeed derived from loss of the TWI1 protein.

TWI1 may work together with other preassembly factors

In addition to the PIH mutants, we also performed spectral counting of dyneins in isolated axonemes from *pf23* (5–4) and *pf22A* (CC-2493) (which contain a wild-type TWI1 gene) and compared to *pf23* (CC-1383) and *pf22* (CC-1382) (which contain a mutation in the TWI1 gene, described above). The dynein defects in *pf23* (CC-1383) are more profound than *pf23* (5–4) (S3A Fig). Particularly, the defects in IDA d (DHC2) and IDA g (DHC7) are larger in *pf23* (CC-1383) than in *pf23* (5–4) [28]. On the other hand, the dynein defects in *pf22A* (CC-2493) and *pf22* (CC-1382) are relatively similar to each other (S3A Fig). In addition to ODAs and IDAs b (DHC5) and c (DHC9) as previously described [16, 32], these *pf22* mutants have large defects ($< 50\%$ of wild-type) in IDAs a (DHC6) and e (DHC8) and minor dyneins DHC3 and DHC4. Also, the axonemal amount of one minor dynein DHC12 is increased in the *pf22* mutants (S3A and S3B Fig). Given that DNAAF4/DYX1C1 (PF23 orthologue) (S1 Table) and DNAAF6/PIH1D3 (TWI1 orthologue) (Table 1) in mammals are predicted to form a complex and work together in dynein preassembly [18], the large dynein defects observed in *pf23* (CC-1383; with *twi1-2* background) may indicate that *Chlamydomonas* TWI1 is needed for efficient function of the PF23 protein in dynein preassembly. Additionally, the swimming phenotype of the *pf23* (CC-1383) strain, rescued with the wild-type PF23 gene, which also harbored the *twi1-2* mutation, was indistinguishable from wild-type [28], consistent with the subtle swimming defect observed in the *twi1-1* mutant.

Discussion

In this report, we characterized two novel PIH preassembly mutants in *Chlamydomonas reinhardtii*, *mot48-2* and *twi1-1*. Although recent studies reveal a conserved role(s) of PIH proteins

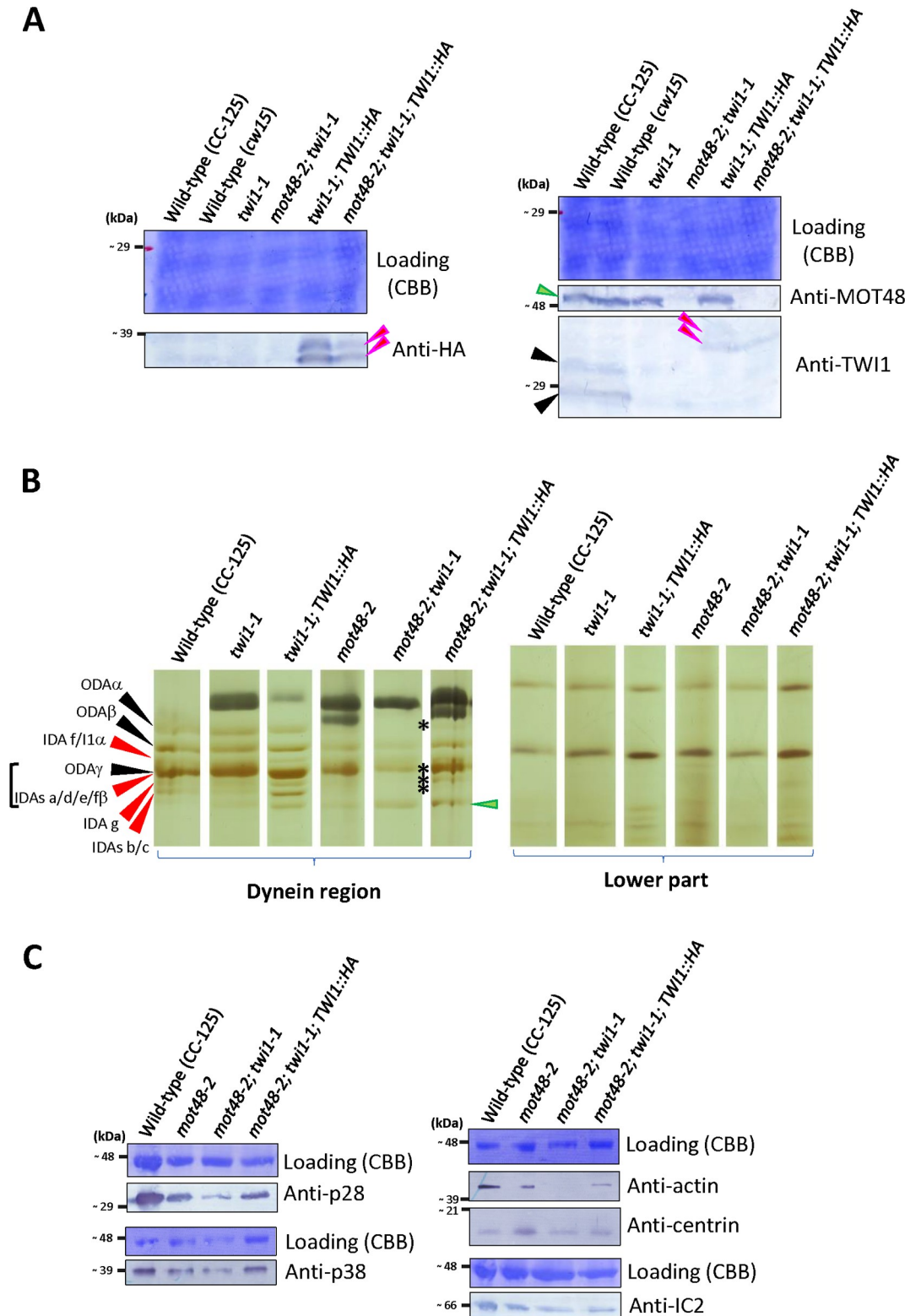


Fig 5. Exogenous TWI1 protein can rescue the *Twi1* phenotype. A) Immunoblot of whole cell samples from wild-type (CC-125 and *cw15*), *twi1-1*, *mot48-2; twi1-1*, *twi1-1; TWI1::HA* and *mot48-2; twi1-1; TWI1::HA* strains using anti-HA (left)/MOT48 and TWI1 (right) antibodies. The black arrowheads indicate the wild-type endogenous TWI1 protein. Red arrowheads indicate the exogenous TWI1 protein with the 3HA tag. The cDNA-driven exogenous TWI1::3HA proteins

show two bands in these blots (red arrowheads). A green arrowhead indicates the MOT48 protein. B) Urea-PAGE of axonemes from wild-type (CC-125), *twi1-1, twi1-1; TWI1::HA, mot48-2, mot48-2; twi1-1*, and *mot48-2; twi1-1; TWI1::HA* strains. For presentation, gel regions of ciliary dyneins and lower parts are shown. The relative positions of ciliary dyneins were adjusted between all strains for comparison. The black arrowheads indicate the HCs of ODA. The red arrowheads indicate the HCs of IDAs. HCs of ODA γ and IDAs a, d, e and f β form a large band in the urea gel. A green arrowhead indicates HC degradation products. In the *mot48-2; twi1-1* strain, the ODA α and IDA bands were missing (asterisks), but these dyneins were recovered in the *mot48-2; twi1-1; TWI1::HA* strain. The correspondence between bands in the Urea-PAGE gel and DHCs was based on [65–67]. C) Immunoblots of axonemal samples from wild-type (CC-125), *mot48-2, mot48-2; twi1-1* and *mot48-2; twi1-1; TWI1::HA* strains using dynein-subunit antibodies (anti-p28/IDA4, p38, actin/IDA5, centrin/VFL2, and IC2/IC69/ODA6; S1 Table).

<https://doi.org/10.1371/journal.pgen.1009126.g005>

in ciliary dynein preassembly [13, 17–19, 21, 22], the specificity of their molecular function(s) and interaction(s) is not fully understood. Our study of assembly of specific dyneins in the axoneme, in the single and double PIH mutants, revealed partially overlapping and specific roles for three *Chlamydomonas* PIH proteins, MOT48, TWI1, and PF13. Accordingly, we have updated our previous model [13] of the preassembly pathway involving PIH proteins and ciliary dynein species (Fig 6). The preassembly pathway of the PIH proteins is more complicated than previously predicted [13], with assembly of each ciliary dynein requiring a specific complement of PIH proteins (Fig 6). We observed assembly defects in some dynein species are more severe in the double preassembly mutants (e.g. *mot48-2; twi1-1, pf13; twi1-1* and *pf23; twi1-2* (CC-1383)) than a single mutant (e.g. *mot48-2, pf13* and *pf23*). In addition, dynein f/II, and possibly IDA a, do not require PIH proteins for assembly (Fig 6 and see [22]). We discuss possibilities in context to the severe phenotypes in the double PIH mutants.

Preassembly of ciliary dyneins likely requires a series of ordered steps each requiring a PIH preassembly protein. For example, full assembly of dynein species IDAs b and c in the axoneme require the activity of at least two PIH proteins including PF13, MOT48 and possibly TWI1 (Figs 4 and 6). Sequential steps in the dynein preassembly have been predicted in previous studies [38–40]. PIH proteins and other preassembly factors may be organized in complexes/organelles such as the DynAP [23] or organized in a series of individual complexes operating in ordered steps (Table 2). Thus, whether in a single complex or in a series of complexes, each PIH protein may operate in a different step in preassembly, and loss of PIH proteins would attenuate the whole preassembly process.

The apparent functional overlap between PIH proteins required for preassembly of certain dyneins, such as IDA c, suggests that the PIH proteins can work with partially overlapping function. Thus, loss of two PIH proteins would cause a more severe phenotype than a single mutation. Consistent with this idea, missing PIH proteins appear to be partially compensated by the other PIH proteins to some extent. For example, the apparent subtle motility defect in *twi1-1* likely derives from a compensatory function of MOT48 and PF13 in the cytoplasm of *twi1-1* cells (see IDA c in Fig 4). This hypothesis is also consistent with our observation that the motility of the *mot48-1/mot48-2* mutant improves as the cells in liquid culture grow old, implying that in the *mot48* cells, PF13 and TWI1 eventually compensate and help to preassemble ciliary dyneins that are usually dependent on MOT48. This idea could explain the occasional ODA assembly in *pf13* axonemes observed by Huang *et al.*, [32]. Predictably, MOT48 and/or TWI1 partially compensate, with time, for PF13 in the *pf13* mutant.

As mentioned above, preassembly factors including PIH proteins, PF22 and PF23 may form in the molecular complex/organelle DynAPs [23]. Based on our data, loss of one subunit protein from this complex may have a modest effect on the activity of the whole complex, but loss of two or more specific subunits largely blocks the activity of the complex for dynein preassembly. Interestingly, in contrast to IDAs b and c, assembly of the minor dyneins, particularly DHC12, only seems to require MOT48. Although we focused on the assembly of dynein

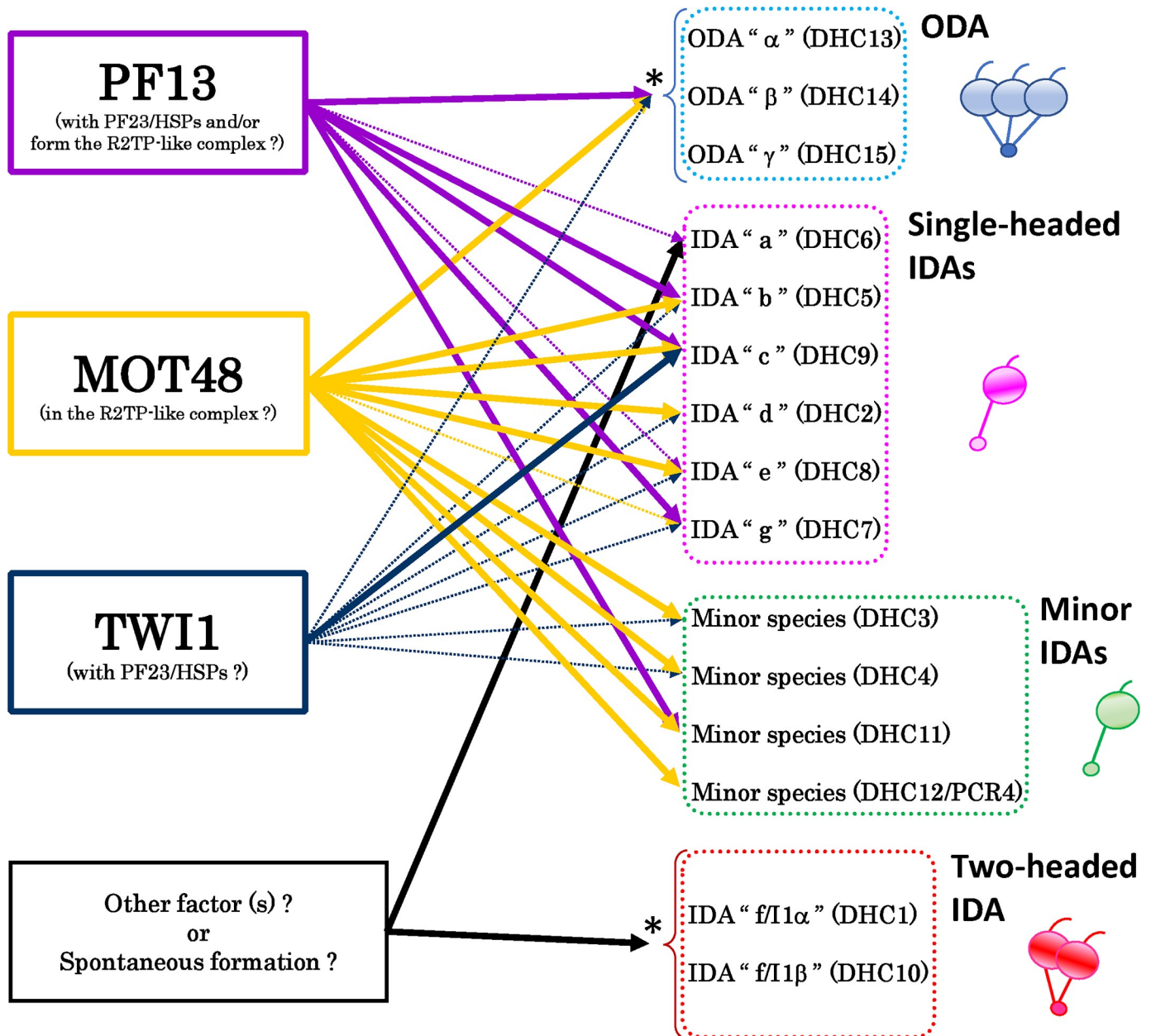


Fig 6. Updated model of the PIH-protein pathways in the dynein preassembly. A proposed model of the functional pathways of PIH preassembly proteins in *Chlamydomonas* adapted from [13]. The bold lines indicate the primary pathways, showing the dynein species that were reduced more than 30% in spectral numbers in each PIH mutant compared to the wild-type. The dotted thin lines indicate relatively secondary pathways, showing the dynein species that were reduced more than 30% in spectral numbers in the double PIH-mutants compared to the single PIH-mutants. The pathways are more complicated than previously thought [13]. Since the three-headed ODA of *Chlamydomonas* cannot be assembled in axonemes in the absence of ODA β or γ HC [68, 69], in this study we could not assess the direct contribution of each PIH protein in the cytoplasmic preassembly of each ODA HC since the amount of ODA α in cilia could be reduced simply in the absence of ODA β or γ HC. Thus, we categorized ODA HCs into one group in this model (asterisk). This is also the case for the two-headed IDA f/I1, in which this species cannot be assembled without each HC (f/I1α or f/I1β)[70, 71], thus we also categorized IDA f/I1 HCs into one group (asterisk). In this study, we could not find any primary pathway of the PIH proteins for the preassembly of IDAs a and f/I1. These dynein species may be preassembled by factors other than PIH proteins (e.g. PF22 or PF23, see S3 Fig), or can assemble spontaneously in cytoplasm to some extent without the help of preassembly factors.

<https://doi.org/10.1371/journal.pgen.1009126.g006>

HCs in the axoneme, we also observed either an increase or decrease in specific LCs in the cytoplasmic compartment. For example, DHC9 (IDA c HC) and p28/IDA4, a LC of several

Table 2. Interacting partners of PIH proteins predicted/identified in previous studies.

Protein Name	Potential Interacting Partner ^a	Reference
PIH1D1/MOT48/IDA10	DNAAF4/DYX1C1	[25]
	HSP90	[18, 40, 41]
	RPAP3	[18, 25, 40–43]
	RuvBL1/Pontin	[18, 25, 40–43]
	RuvBL2/Reptin	[18, 25, 40–43]
	WDR92/Monad	[25, 40, 43]
PIH1D2	HSP70	[27]
	HSP90	[27]
	SPAG1	[42, 43]
	RuvBL1/Pontin	[42, 43]
	RuvBL2/Reptin	[42, 43]
DNAAF6/PIH1D3/Twister/TWI1	DNAAF4/DYX1C1	[18, 19, 40, 42, 43]
	DNAAF2/KTU/PF13	[19]
	HSP70	[21]
	HSP90	[18, 21]
DNAAF2/KTU/PF13	DNAAF4/DYX1C1	[18, 40, 42, 43]
	HSP70	[17]
	HSP90	[18]
	RuvBL1/Pontin	[18, 43]
	RuvBL2/Reptin	[18, 43]
	SPAG1	[42, 43]

^a Potential interacting partners of PIH proteins predicted/identified in various organisms are summarized in one table.

<https://doi.org/10.1371/journal.pgen.1009126.t002>

single-headed IDAs, are reduced in the cytoplasm of PIH mutants with the *mot48* background (Fig 3E, see also [13]). In addition, actin/IDA5, another LC of single-headed dyneins, accumulates in the cytoplasm of PIH mutants with the *pf13* and/or *mot48-2* background (Fig 3E). Thus, stability of dynein subunits in the cytoplasm may offer another approach toward understanding PIH protein function. One model is that the PIH proteins play roles in the folding and stability of dynein HCs, and also in the following LC assembly to HC [17–19, 21, 40]. Further biochemical analyses, in combination with the *in vitro* reconstitution, are required to define the details of PIH protein function.

Although *Chlamydomonas* MOT48 was first identified as a protein that is conserved in organisms with motile cilia [44], an exact orthologous *MOT48* gene in vertebrates remains unclear. A recent study showed that among the four PIH proteins found in vertebrates, PIH1D1, PIH1D2, DNAAF6/PIH1D3 (TWI1 orthologue), and DNAAF2/KTU (PF13 orthologue), MOT48 groups near DNAAF2/KTU and PIH1D1 in a phylogenetic tree [22]. We also generated a phylogenetic tree using the full-length sequences of PIH proteins (S4 Fig), and also found that MOT48 fell into a group with PIH1D1 proteins. A BLAST search against the NCBI database (<https://blast.ncbi.nlm.nih.gov/Blast.cgi>) also revealed that among the four PIH proteins in vertebrates, PIH1D1 showed the highest similarity to MOT48, although the E-values were relatively low (< 7E-15). In addition, recently MOT48 has been reported to interact with RPAP3 and RuvBL1 [25], components of the known R2TP chaperone complex [41] to form a potential R2TP-like complex in *Chlamydomonas* cytoplasm (Table 2). Thus, MOT48 may have a function as a co-factor in the *Chlamydomonas* R2TP-like complex, which is similar to the PIH1D1 function in higher eukaryotes [41].

The TWI1 orthologue, DNAAF6/PIH1D3, has also been postulated to interact with DNAAF4/DYX1C1 [18], orthologous to the PF23 protein in *Chlamydomonas* [28]. Thus, TWI1 may function as part of a large chaperone complex [18, 19, 23](Table 2). Using the 3HA-tagged rescued strains (*mot48-2*; *MOT48::HA* and *twi1-1*; *TWI1::HA*) for identification of interacting partners, we failed to identify chaperone related proteins. This negative result could indicate weak and/or transient interactions of the PIH proteins with chaperones and/or interacting partners of MOT48 and TWI1. Further structural and biochemical studies of PIH interacting proteins, including specific dynein HC/IC/LCs, are required for understanding assembly complexes, steps and specificity of each PIH protein required for ciliary dynein assembly.

Summary

The mechanisms for PIH proteins in assembly of ciliary dyneins are more complicated than previously thought. *Chlamydomonas* uses the three PIH proteins, MOT48, TWI1, and PF13, for ciliary dynein preassembly. Based on analysis in single and double PIH mutants, specific PIH proteins are required for assembly of specific dyneins, in some cases, and in other cases the PIH proteins can work in partially overlapping fashion. Further biochemical studies, and the two novel *Chlamydomonas* PIH preassembly mutants, *mot48-2* and *twi1-1*, from this study, will define our understanding of dynein assembly.

Materials and methods

Chlamydomonas strains and samples

The *Chlamydomonas* strains used in this study are listed in S2 Table. The novel *mot48* (*ida10*) allele, referred to as *mot48-2* was isolated from a CLiP library strain (LMJ.RY0402.055540)[24] having a mutation that was unlinked to the paromomycin resistant (*APHVIII*) insertional cassette used for selection but caused a slow-swimming phenotype. The original LMJ.RY0402.055540 strain was backcrossed with the wild-type (CC-125) strain to separate this mutation, and two *mot48-2* progeny were isolated. The identification of the *mot48* background was confirmed by Sanger sequencing using the primer pair: *Ida10-2* GF2 (5'-TGGCAGCACATTC ATAAGCA-3') and *Ida10-2* GR2 (5'-CGCTGTACTAGAGCCCCCTCA-3'). The *twi1* strain was first obtained from the CLiP library (LMJ.RY0402.076787)[24] and backcrossed with the wild-type strain (CC-125), and the *twi1* mutant progeny (*twi1-1*) were used for experiments. Cells were grown in the tris-acetic acid-phosphate (TAP) liquid/solid media as previously described [45]. Double *Chlamydomonas* PIH mutants were obtained using the standard tetrad procedure [45]. The deciliation was performed following the standard procedure [46]. For preparation of whole cell samples or de-ciliated cell-body samples, whole cells/cell bodies were extracted with water/methanol/chloroform (volume ratio = 3:4:1) to remove the nucleic acids, lipids and chlorophyll, and the denatured proteins were boiled in the SDS-sample buffer as previously described [47].

Rescue of *mot48-2*, *twi1-1*, and *mot48-2*; *twi1-1*

Phenotypic rescue of the *mot48-2*, *twi1-1*, and *mot48-2*; *twi1-1* strains was performed by the electroporation method using each wild-type gene cloned in the modified pGend vector (pGend-MCS-3HA-AphVIII/pGend-MCS-mCherry-3HA-AphVIII/pGend-MCS-3HA-Hyg) [13, 48, 49]. The rescued strain, *mot48-2*; *MOT48::HA* expressed exogenous MOT48 with a 3HA tag at the C-terminus. The rescued strain, *mot48-2*; *MOT48::mCherry-HA* expressed exogenous MOT48 with the mCherry-3HA tag at the C-terminus. The pGend-MOT48-

3HA-AphVIII vector was previously described [13] and also used in this study. The two *twi1-1* rescued strains, *twi1-1; TWI1::HA* and *mot48-2; twi1-1; TWI1::HA* expressed exogenous TWI1 with a 3HA tag at the C-terminus. The primer pair used for wild-type *TWI1* cloning was as follows, TWI1-pGend-F1 (5'-CACAAACAAGCCCATATGGACATTGGGAGCTTCACTGCTGA-3') and TWI1-pGend-R1 (5'-GGTATCGATCGAATTCGAATGGCTCTTCCCGAATGATGCG-3'). The NdeI/EcoRI sites used for cloning are underlined.

Spectral counting analysis

A semi-quantitative estimation of the amount of dyneins in the isolated axonemes [28, 50, 51] was conducted using the spectral counting analyses on some LC-MS/MS spectrometers at University of Massachusetts Medical School Mass Spectrometry Facility.

A first set of experiments was performed on dyneins from the wild-type (CC-124, *cw15*), *mot48-1*, and *mot48-2* strains with the aim of comparing the dynein levels between the *mot48-1* and *mot48-2* strains. For normalization and comparison between samples, the peptide numbers of ciliary dyneins observed in the CC-124 strain were assigned a ratio of 1.0, and the observed peptide numbers of Hydin [52], a central-pair protein were also used as an internal standard. The first-set of experiments was generously performed by Dr. John Leszyk (University of Massachusetts Medical School). Thresholds in the Scaffold 4 software (<http://www.proteomesoftware.com/products/scaffold/>) for the first-set of analyses were set as follows: Protein Threshold: 90%/Minimal Peptides Number: 2/ Peptide Threshold: 70%. The averages of two independent experiments are summarized in Fig 2.

A second set of experiments was performed on dyneins from wild-type (CC-125), *twi1-1*, *mot48-2*, *mot48-2; twi1-1, pf13, pf13; twi1-1*, and *pf23* (5–4) strains with the aim of comparing the dynein levels between the single and double PIH preassembly mutants. For normalization and comparison between samples, observed peptide numbers in the CC-125 strain and also the peptide numbers of Hydin were used. The second set of experiments was generously performed by Drs. Scott Shaffer and Xuni Li (University of Massachusetts Medical School). Thresholds in the Scaffold 4 software for the second-set analyses were set as follows: Protein Threshold: 99%/Minimal Peptides Number: 2/ Peptide Threshold: 70%. The results are summarized in Fig 4 and S3 Fig.

A third set of experiments was performed on dyneins from wild-type (CC-125), *twi1-1; TWI1::HA*, *pf22* (CC-1382 with the *twi1-2* background) and *pf22A* (CC-2493) strains with the aim to check the dynein rescue and effect of the *twi1-2* mutation in dynein assembly in *pf22* strains. Observed peptide numbers were normalized using peptide numbers of CC-125 and Hydin, and the results were combined/incorporated into Fig 4 and S3 Fig. The third set of experiments was generously performed by Drs. Scott Shaffer and Roshanak Aslebagh (University of Massachusetts Medical School). Thresholds in the Scaffold 4 software for the third-set analyses were set as follows: Protein Threshold: 99%/Minimal Peptides Number: 2/ Peptide Threshold: 77%. The spectral counting data of *pf23* (CC-1383 with the *twi1-2* background) normalized with the wild-type (137c) peptide counts were reanalyzed/refined from our previous paper [28] with the Hydin normalization in S3 Fig.

TWI1 antibody production

The TWI1 cDNA sequence was determined using the *Chlamydomonas* cDNA library (*Chlamydomonas* Resource Center) and cloned into the NdeI/BamHI site of the pET15b vector (Novagen) by the In-Fusion HD Cloning enzyme (TAKARA). The primer pair to amplify the TWI1 cDNA sequence was as follows: TWI1-CF1 (5'-CGCGCGGCAGCCATATGGACATTGGGAGCTTCACTG-3') and TWI1-CR1 (5'-GTTAGCAGCCGGATCCGAATGGCTCT

TCCCGAATGATGCG-3')(The NdeI/BamHI sites are underlined). The purified TWI1 protein with a 6His tag at the N-terminus was used as antigen to immunize two rabbits. The antisera from rabbits were blot and Protein-A purified before use, as previously described [53, 54]. The *Chlamydomonas TWI1* cDNA sequence determined in this study was deposited in the DNA Data Bank of Japan (DDBJ) under the accession No. LC461993.

Other methods

SDS-PAGE and immunoblotting were performed following standard procedures [55, 56]. For the immunoblotting, antibodies used included: primary antibodies (anti-MOT48 [28], anti-HA (Y-11)(Santa Cruz), anti-HA (3F10)-HRP (Roche), anti-PF23 [28], anti-TWI1 (this study), anti-actin/IDA5 [57], anti-p28/IDA4 [58], anti-centrin/VFL2 (20H5)(MilliporeSigma), anti-p38 [59], anti-IC138/BOP5 [60], anti-IC2/IC69/ODA6 [61], anti-DHC9 (IDA c HC) [37]); secondary antibody (Goat-anti-Rabbit or Mouse-HRP (Roche)). Immunofluorescent microscopic observation of nucleo-flagellar apparatuses was performed as described previously [36, 37, 62], and the acquired images were adjusted for presentation using Photoshop (Adobe). The urea PAGE used to resolve ciliary dynein bands was performed as previously described [63]. The swimming velocity of *Chlamydomonas* was assessed on free-swimming cells in liquid culture using our in-lab video system and ImageJ software (<https://www.google.com/search?client=firefox-b-d&q=imagej+software>) [64]. Velocities were measured on the 3-day liquid cultured cells, and reported in the text as average \pm standard deviation. The ciliated cell ratio in the *pf13* and *pf13; twi1-1* strains was counted and averaged on three days. Student's t-test was performed on Excel (Microsoft).

Supporting information

S1 Fig. Swimming velocity measurement of *mot48-2/twi1-1*-related strains. Swimming velocities of wild-type (CC-125), *mot48-2*, *mot48-2; MOT48::HA*, *mot48-2; MOT48::mCherry-HA*, *twi1-1*, *twi1-1; TWI1::HA*, *mot48-2; twi1-1*, and *mot48-2; twi1-1; TWI1::HA*. For wild-type (CC-125), *twi1-1*, *twi1-1; TWI1::HA*, *mot48-2; MOT48::HA*, and *mot48-2; MOT48::mCherry-HA*, more than 40 cells were measured. For *mot48-2*, *mot48-2; twi1-1*, and *mot48-2; twi1-1; TWI1::HA*, it was difficult to find ideal cells for the velocity measurement, but more than 15 cells were measured. As discussed in the main text, the swimming phenotypes of the preassembly mutants slightly varied from day to day and culture to culture because of the apparent compensatory and overlapping nature of the dynein preassembly. In this figure, swimming velocities are shown for cells cultured for 3 days in the liquid TAP media in mini petri-dishes under constant light. Asterisks indicate $p < 0.01$ in the Student's t-test. (TIF)

S2 Fig. Immunofluorescent microscopic observation of ciliary dyneins in axonemes from PIH mutants. Immunofluorescence localization of DHC9 (IDA c HC), DHC11 (minor dynein HC) and α -tubulin in wild-type (CC-124), *pf13* and *mot48-2* nucleo-flagellar apparatuses. DHC11 was shown to be localized at the proximal part of the wild-type axonemes [37]. Both DHC9 and DHC11 signals were reduced in the *pf13* and *mot48-2* axonemes compared to wild-type axonemes. The bright puncta are non-specific staining/autofluorescence. Bar: $\sim 5 \mu\text{m}$. (TIF)

S3 Fig. Dynein defects are more severe in the *pf23* mutant also containing the *twi1-2* mutation. A) Spectral counting comparison of dyneins from axonemes of *pf23* (5–4), *pf23* (CC-1383; with the *twi1-2* background), *pf22A* (CC-2493), and *pf22* (CC-1382; with the *twi1-2*

background). The spectral data of *pf23* (5–4) are from the second set of experiments. The spectral data of *pf22A* (CC-2493) and *pf22* (CC-1382) are from the third set of experiments. The spectral data of *pf23* (CC-1383) are refined/reanalyzed from our previous study [28]. The spectral numbers observed in the mutants were normalized using the spectral numbers of Hydin and wild-type peptides (CC-125 for *pf23* (5–4), *pf22A* (CC-2493), and *pf22* (CC-1382), and 137c for *pf23* (CC-1383)[28]). Asterisks indicate the ciliary dynein species for which the spectral numbers in the *pf23* strain (CC-1383; with the *twi1-2* background) showed more than a 50% reduction compared to the *pf23* (5–4) strain. **B**) Ciliary dynein species for which the spectral numbers in the *pf23* (5–4) or *pf22A* (CC-2493) strain (without the *twi1-2* background) showed a more than 50% reduction compared to wild-type (CC-125) are summarized. (TIF)

S4 Fig. Phylogenetic analysis of PIH proteins from *Chlamydomonas reinhardtii* and other organisms. The protein alignment was performed using the ClustalW software (v2.1)(<http://clustalw.ddbj.nig.ac.jp/>) by the default settings, and the phylogenetic tree was drawn by the Neighbor-Joining method [72] and modified in MEGA7 program (<https://www.megasoftware.net/>). The bootstrap consensus tree inferred from 1000 replicates is shown, and the bootstrap numbers are shown in percentile [73]. The evolutionary distances were computed using the p-distance method [74], and all positions containing gaps and missing data were eliminated. The DNAAF4/DYX1C1/PF23 proteins, which have the CS (CHORD-containing proteins and SGT1) domain relating to the PIH1 domain [18] were used as an out-group. In this tree, *Chlamydomonas* MOT48 falls into the PIH1D1 group. The accession numbers of proteins used to draw this tree were as follows: Human DNAAF2/KTU (NCBI: ACN30493.1); Mouse DNAAF2/KTU (NCBI: NP_081545.3); Zebrafish KTU (NCBI: NP_001028272.1); *Chlamydomonas* PF13 (NCBI: BAG69288.1); Human PIH1D1 (NCBI: NP_060386.1); Mouse PIH1D1 (NCBI: AAH68254.1); Zebrafish PIH1D1 (NCBI: NP_001153400.1); Human PIH1D2 (NCBI: AAH19238.1); Mouse PIH1D2 (NCBI: AAH39645.1); Zebrafish PIH1D2 (NCBI: NP_001008629.1); *Chlamydomonas* MOT48 (NCBI: BAI83444.1); Human DNAAF6/PIH1D3 (NCBI: NP_001162625.1); Mouse DNAAF6a/PIH1D3a (NCBI: NP_083338.1); Mouse DNAAF6b/PIH1D3b/Twister2 (NCBI: AAI19079.1) [21]; Zebrafish Twister (NCBI: NP_001002309.1); *Chlamydomonas* TWI1 (NCBI: LC461993, This study); Human DNAAF4/DYX1C1 (NCBI: NP_570722.2); Mouse DNAAF4/DYX1C1 (NCBI: NP_080590.3); Zebrafish DNAAF4/DYX1C1 (NCBI: NP_991251.1); *Chlamydomonas* PF23 (NCBI: BBA27223.1); Yeast Nop17 (NCBI: GAX71541.1). (TIF)

S1 Table. *Chlamydomonas* dynein subunits, IFT proteins, and non-PIH preassembly proteins mentioned in this study and their potential human orthologues. (PDF)

S2 Table. *Chlamydomonas* strains used in this study. (PDF)

Acknowledgments

We thank Drs. John Leszyk, Xuni Li, Roshanak Aslebagh, and Scott Shaffer (The University of Massachusetts Medical School) for kindly performing the spectral counting analyses on ciliary axonemal dyneins. We thank Dr. Ritsu Kamiya (Chuo University) for kindly performing the backcross of the *mot48-2* strain.

Author Contributions

Conceptualization: Ryosuke Yamamoto, Takahide Kon.

Data curation: Ryosuke Yamamoto, Shiho Yanagi, Masahito Nagao, Yuya Yamasaki, Yui Tanaka, Toshiki Yagi.

Funding acquisition: Ryosuke Yamamoto, Winfield S. Sale, Toshiki Yagi, Takahide Kon.

Investigation: Ryosuke Yamamoto, Shiho Yanagi, Masahito Nagao, Yuya Yamasaki, Yui Tanaka, Toshiki Yagi.

Supervision: Takahide Kon.

Validation: Winfield S. Sale.

Writing – original draft: Ryosuke Yamamoto, Takahide Kon.

Writing – review & editing: Winfield S. Sale, Toshiki Yagi.

References

1. Ishikawa T. Axoneme Structure from Motile Cilia. *Cold Spring Harb Perspect Biol.* 2017; 9(1):a028076. <https://doi.org/10.1101/cshperspect.a028076> PMID: 27601632
2. Satir P. CILIA: before and after. *Cilia.* 2017; 6:1. <https://doi.org/10.1186/s13630-017-0046-8> PMID: 28293419
3. Zariwala MA, Omran H, Ferkol TW. The emerging genetics of primary ciliary dyskinesia. *Proc Am Thorac Soc.* 2011; 8(5):430–3. <https://doi.org/10.1513/pats.201103-023SD> PMID: 21926394
4. Chodhari R, Mitchison HM, Meeks M. Cilia, primary ciliary dyskinesia and molecular genetics. *Paediatr Respir Rev.* 2004; 5(1):69–76. <https://doi.org/10.1016/j.prrv.2003.09.005> PMID: 15222957
5. Rubbo B, Lucas JS. Clinical care for primary ciliary dyskinesia: current challenges and future directions. *Eur Respir Rev.* 2017; 26(145):170023. <https://doi.org/10.1183/16000617.0023-2017> PMID: 28877972
6. Horani A, Ferkol TW. Advances in the Genetics of Primary Ciliary Dyskinesia: Clinical Implications. *Chest.* 2018; 154(3):645–52. <https://doi.org/10.1016/j.chest.2018.05.007> PMID: 29800551
7. Viswanadha R, Sale WS, Porter ME. Ciliary Motility: Regulation of Axonemal Dynein Motors. *Cold Spring Harb Perspect Biol.* 2017; 9(8):a018325. <https://doi.org/10.1101/cshperspect.a018325> PMID: 28765157
8. Kamiya R, Yagi T. Functional diversity of axonemal dyneins as assessed by in vitro and in vivo motility assays of *Chlamydomonas* mutants. *Zoolog Sci.* 2014; 31(10):633–44. <https://doi.org/10.2108/zs140066> PMID: 25284382
9. King SM. Axonemal Dynein Arms. *Cold Spring Harb Perspect Biol.* 2016; 8(11):a028100. <https://doi.org/10.1101/cshperspect.a028100> PMID: 27527589
10. Brokaw CJ, Kamiya R. Bending patterns of *Chlamydomonas* flagella: IV. Mutants with defects in inner and outer dynein arms indicate differences in dynein arm function. *Cell Motil Cytoskeleton.* 1987; 8(1):68–75. <https://doi.org/10.1002/cm.970080110> PMID: 2958145
11. Fowkes ME, Mitchell DR. The role of preassembled cytoplasmic complexes in assembly of flagellar dynein subunits. *Mol Biol Cell.* 1998; 9(9):2337–47. <https://doi.org/10.1091/mbc.9.9.2337> PMID: 9725897
12. Viswanadha R, Hunter EL, Yamamoto R, Wirschell M, Alford LM, Dutcher SK, et al. The ciliary inner dynein arm, I1 dynein, is assembled in the cytoplasm and transported by IFT before axonemal docking. *Cytoskeleton (Hoboken).* 2014; 71(10):573–86. <https://doi.org/10.1002/cm.21192> PMID: 25252184
13. Yamamoto R, Hirono M, Kamiya R. Discrete PIH proteins function in the cytoplasmic preassembly of different subsets of axonemal dyneins. *J Cell Biol.* 2010; 190(1):65–71. <https://doi.org/10.1083/jcb.201002081> PMID: 20603327
14. Kobayashi D, Takeda H. Ciliary motility: the components and cytoplasmic preassembly mechanisms of the axonemal dyneins. *Differentiation.* 2012; 83(2):S23–9. <https://doi.org/10.1016/j.diff.2011.11.009> PMID: 22154137
15. Desai PB, Dean AB, Mitchell DR. Cytoplasmic preassembly and trafficking of axonemal dyneins: Dyneins (The Biology of Dynein Motors). 2nd Edition ed: Academic Press; 2017. 684 p.

16. Mitchison HM, Schmidts M, Loges NT, Freshour J, Dritsoula A, Hirst RA, et al. Mutations in axonemal dynein assembly factor DNAAF3 cause primary ciliary dyskinesia. *Nat Genet.* 2012; 44(4):381–9, s1-2. <https://doi.org/10.1038/ng.1106> PMID: 22387996
17. Omran H, Kobayashi D, Olbrich H, Tsukahara T, Loges NT, Hagiwara H, et al. Ktu/PF13 is required for cytoplasmic pre-assembly of axonemal dyneins. *Nature.* 2008; 456(7222):611–16. <https://doi.org/10.1038/nature07471> PMID: 19052621
18. Olcese C, Patel MP, Shoemark A, Kiviluoto S, Legendre M, Williams HJ, et al. X-linked primary ciliary dyskinesia due to mutations in the cytoplasmic axonemal dynein assembly factor PIH1D3. *Nat Commun.* 2017; 8:14279. <https://doi.org/10.1038/ncomms14279> PMID: 28176794
19. Paff T, Loges NT, Aprea I, Wu K, Bakey Z, Haarman EG, et al. Mutations in PIH1D3 cause X-linked primary ciliary dyskinesia with outer and inner dynein arm defects. *Am J Hum Genet.* 2017; 100(1):160–8. <https://doi.org/10.1016/j.ajhg.2016.11.019> PMID: 28041644
20. Tarkar A, Loges NT, Slagle CE, Francis R, Dougherty GW, Tamayo JV, et al. DYX1C1 is required for axonemal dynein assembly and ciliary motility. *Nat Genet.* 2013; 45(9):995–1003. <https://doi.org/10.1038/ng.2707> PMID: 23872636
21. Dong F, Shinohara K, Botilde Y, Nabeshima R, Asai Y, Fukumoto A, et al. Pih1d3 is required for cytoplasmic preassembly of axonemal dynein in mouse sperm. *J Cell Biol.* 2014; 204(2):203–13. <https://doi.org/10.1083/jcb.201304076> PMID: 24421334
22. Yamaguchi H, Oda T, Kikkawa M, Takeda H. Systematic studies of all PIH proteins in zebrafish reveal their distinct roles in axonemal dynein assembly. *Elife.* 2018; 7:e36979. <https://doi.org/10.7554/eLife.36979> PMID: 29741156
23. Huizar RL, Lee C, Boulgakov AA, Horani A, Tu F, Marcotte EM, et al. A liquid-like organelle at the root of motile ciliopathy. *Elife.* 2018; 7:e38497. <https://doi.org/10.7554/eLife.38497> PMID: 30561330
24. Li X, Zhang R, Patena W, Gang SS, Blum SR, Ivanova N, et al. An indexed, mapped mutant library enables reverse genetics studies of biological processes in *Chlamydomonas reinhardtii*. *Plant Cell.* 2016; 28(2):367–87. <https://doi.org/10.1105/tpc.15.00465> PMID: 26764374
25. Liu G, Wang L, Pan J. *Chlamydomonas* WDR92 in association with R2TP-like complex and multiple DNAAFs to regulate ciliary dynein preassembly. *J Mol Cell Biol.* 2019; 11(9):770–80. <https://doi.org/10.1093/jmcb/mjy067> PMID: 30428028
26. Hom EF, Witman GB, Harris EH, Dutcher SK, Kamiya R, Mitchell DR, et al. A unified taxonomy for ciliary dyneins. *Cytoskeleton (Hoboken).* 2011; 68(10):555–65. <https://doi.org/10.1002/cm.20533> PMID: 21953912
27. Fabczak H, Osinka A. Role of the novel Hsp90 co-chaperones in dynein arms' preassembly. *Int J Mol Sci.* 2019; 20(24):6174. <https://doi.org/10.3390/ijms20246174> PMID: 31817850
28. Yamamoto R, Obbineni JM, Alford LM, Ide T, Owa M, Hwang J, et al. *Chlamydomonas* DYX1C1/PF23 is essential for axonemal assembly and proper morphology of inner dynein arms. *PLoS Genet.* 2017; 13(9):e1006996. <https://doi.org/10.1371/journal.pgen.1006996> PMID: 28892495
29. Zhao R, Kakihara Y, Gribun A, Huen J, Yang G, Khanna M, et al. Molecular chaperone Hsp90 stabilizes Pih1/Nop17 to maintain R2TP complex activity that regulates snoRNA accumulation. *J Cell Biol.* 2008; 180(3):563–78. <https://doi.org/10.1083/jcb.200709061> PMID: 18268103
30. Pal M, Morgan M, Phelps SEL, Roe SM, Parry-Morris S, Downs JA, et al. Structural basis for phosphorylation-dependent recruitment of Tel2 to Hsp90 by Pih1. *Structure (London, England: 1993).* 2014; 22(6):805–18. <https://doi.org/10.1016/j.str.2014.04.001> PMID: 24794838
31. King SM. 7—Composition and Assembly of Axonemal Dyneins. In: King SM, editor. *Dyneins*. Boston: Academic Press; 2012. p. 208–43.
32. Huang B, Piperno G, Luck DJ. Paralyzed flagella mutants of *Chlamydomonas reinhardtii*. Defective for axonemal doublet microtubule arms. *J Biol Chem.* 1979; 254(8):3091–9. PMID: 429335
33. Stolc V, Samanta MP, Tongprasit W, Marshall WF. Genome-wide transcriptional analysis of flagellar regeneration in *Chlamydomonas reinhardtii* identifies orthologs of ciliary disease genes. *Proc Natl Acad Sci U S A.* 2005; 102(10):3703–7. <https://doi.org/10.1073/pnas.0408358102> PMID: 15738400
34. King SM, Patel-King RS. The oligomeric outer dynein arm assembly factor CCDC103 is tightly integrated within the ciliary axoneme and exhibits periodic binding to microtubules. *J Biol Chem.* 2015; 290(12):7388–401. <https://doi.org/10.1074/jbc.M114.616425> PMID: 25572396
35. Kim KS, Kustu S, Inwood W. Natural history of transposition in the green alga *Chlamydomonas reinhardtii*: use of the AMT4 locus as an experimental system. *Genetics.* 2006; 173(4):2005–19. <https://doi.org/10.1534/genetics.106.058263> PMID: 16702425
36. Bui KH, Yagi T, Yamamoto R, Kamiya R, Ishikawa T. Polarity and asymmetry in the arrangement of dynein and related structures in the *Chlamydomonas* axoneme. *J Cell Biol.* 2012; 198(5):913–25. <https://doi.org/10.1083/jcb.201201120> PMID: 22945936

37. Yagi T, Uematsu K, Liu Z, Kamiya R. Identification of dyneins that localize exclusively to the proximal portion of *Chlamydomonas* flagella. *J Cell Sci*. 2009; 122(9):1306–14. <https://doi.org/10.1242/jcs.045096> PMID: 19351714
38. Horani A, Ustione A, Huang T, Firth AL, Pan J, Gunsten SP, et al. Establishment of the early cilia preassembly protein complex during motile ciliogenesis. *Proc Natl Acad Sci U S A*. 2018; 115(6):E1221–28. <https://doi.org/10.1073/pnas.1715915115> PMID: 29358401
39. Mali GR, Yeyati PL, Mizuno S, Dodd DO, Tennant PA, Keighren MA, et al. ZMYND10 functions in a chaperone relay during axonemal dynein assembly. *Elife*. 2018; 7:e34389. <https://doi.org/10.7554/eLife.34389> PMID: 29916806
40. Zur Lage P, Stefanopoulou P, Styczynska-Soczka K, Quinn N, Mali G, von Kriegsheim A, et al. Ciliary dynein motor preassembly is regulated by Wdr92 in association with HSP90 co-chaperone, R2TP. *J Cell Biol*. 2018; 217(7):2583–98. <https://doi.org/10.1083/jcb.201709026> PMID: 29743191
41. Kakahara Y, Houry WA. The R2TP complex: discovery and functions. *Biochim Biophys Acta*. 2012; 1823(1):101–7. <https://doi.org/10.1016/j.bbamcr.2011.08.016> PMID: 21925213
42. Maurizy C, Quinternet M, Abel Y, Verheggen C, Santo PE, Bourguet M, et al. The RPAP3-Cterminal domain identifies R2TP-like quaternary chaperones. *Nat Commun*. 2018; 9(1):2093. <https://doi.org/10.1038/s41467-018-04431-1> PMID: 29844425
43. Patel-King RS, Sakato-Antoku M, Yankova M, King SM. WDR92 is required for axonemal dynein heavy chain stability in cytoplasm. *Mol Biol Cell*. 2019; 30(15):1834–45. <https://doi.org/10.1091/mbc.E19-03-0139> PMID: 31116681
44. Merchant SS, Prochnik SE, Vallon O, Harris EH, Karpowicz SJ, Witman GB, et al. The *Chlamydomonas* genome reveals the evolution of key animal and plant functions. *Science*. 2007; 318(5848):245–50. <https://doi.org/10.1126/science.1143609> PMID: 17932292
45. Harris EH. The *Chlamydomonas* sourcebook: a comprehensive guide to biology and laboratory use: Academic Press, San Diego, 780pp; 1989.
46. Craige B, Brown JM, Witman GB. Isolation of *Chlamydomonas* flagella. *Curr Protoc Cell Biol*. 2013; Chapter 3:Unit 3.41.1–9. <https://doi.org/10.1002/0471143030.cb0341s59> PMID: 23728744
47. Bölling C, Fiehn O. Metabolite profiling of *Chlamydomonas reinhardtii* under nutrient deprivation. *Plant Physiol*. 2005; 139(4):1995–2005. <https://doi.org/10.1104/pp.105.071589> PMID: 16306140
48. Shimogawara K, Fujiwara S, Grossman A, Usuda H. High-efficiency transformation of *Chlamydomonas reinhardtii* by electroporation. *Genetics*. 1998; 148(4):1821–8. PMID: 9560396
49. Fischer N, Rochaix JD. The flanking regions of *PsaD* drive efficient gene expression in the nucleus of the green alga *Chlamydomonas reinhardtii*. *Mol Genet Genomics*. 2001; 265(5):888–94. <https://doi.org/10.1007/s004380100485> PMID: 11523806
50. Wirschell M, Olbrich H, Werner C, Tritschler D, Bower R, Sale WS, et al. The nexin-dynein regulatory complex subunit DRC1 is essential for motile cilia function in algae and humans. *Nat Genet*. 2013; 45(3):262–8. <https://doi.org/10.1038/ng.2533> PMID: 23354437
51. Lin J, Le TV, Augspurger K, Tritschler D, Bower R, Fu G, et al. FAP57/WDR65 targets assembly of a subset of inner arm dyneins and connects to regulatory hubs in cilia. *Mol Biol Cell*. 2019; 30(21):2659–80. <https://doi.org/10.1091/mbc.E19-07-0367> PMID: 31483737
52. Lechtreck KF, Witman GB. *Chlamydomonas reinhardtii* hidin is a central pair protein required for flagellar motility. *J Cell Biol*. 2007; 176(4):473–82. <https://doi.org/10.1083/jcb.200611115> PMID: 17296796
53. Tang W-JY. Chapter 5 Blot-Affinity Purification of Antibodies. In: Asai DJ, editor. *Methods Cell Biol*. 37: Academic Press; 1993. p. 95–104. [https://doi.org/10.1016/s0091-679x\(08\)60245-9](https://doi.org/10.1016/s0091-679x(08)60245-9) PMID: 8255253
54. Grodzki AC, Berenstein E. Antibody purification: affinity chromatography—protein A and protein G Sepharose. *Methods Mol Biol*. 2010; 588:33–41. https://doi.org/10.1007/978-1-59745-324-0_5 PMID: 20012816
55. Laemmli UK. Cleavage of structural proteins during the assembly of the head of bacteriophage T4. *Nature*. 1970; 227(5259):680–5. <https://doi.org/10.1038/227680a0> PMID: 5432063
56. Kurien BT, Scofield RH. Western blotting. *Methods*. 2006; 38(4):283–93. <https://doi.org/10.1016/j.ymeth.2005.11.007> PMID: 16483794
57. Kato-Minoura T, Hirono M, Kamiya R. *Chlamydomonas* inner-arm dynein mutant, *ida5*, has a mutation in an actin-encoding gene. *J Cell Biol*. 1997; 137(3):649–56. <https://doi.org/10.1083/jcb.137.3.649> PMID: 9151671
58. LeDizet M, Piperno G. The light chain p28 associates with a subset of inner dynein arm heavy chains in *Chlamydomonas* axonemes. *Mol Biol Cell*. 1995; 6(6):697–711. <https://doi.org/10.1091/mbc.6.6.697> PMID: 7579689

59. Yamamoto R, Yanagisawa HA, Yagi T, Kamiya R. A novel subunit of axonemal dynein conserved among lower and higher eukaryotes. *FEBS Lett.* 2006; 580(27):6357–60. <https://doi.org/10.1016/j.febslet.2006.10.047> PMID: 17094970
60. Hendrickson TW, Perrone CA, Griffin P, Wuichet K, Mueller J, Yang P, et al. IC138 is a WD-repeat dynein intermediate chain required for light chain assembly and regulation of flagellar bending. *Mol Biol Cell.* 2004; 15(12):5431–42. <https://doi.org/10.1091/mbc.e04-08-0694> PMID: 15469982
61. King SM, Otter T, Witman GB. Characterization of monoclonal antibodies against *Chlamydomonas* flagellar dyneins by high-resolution protein blotting. *Proc Natl Acad Sci U S A.* 1985; 82(14):4717–21. <https://doi.org/10.1073/pnas.82.14.4717> PMID: 3161075
62. Sanders MA, Salisbury JL. Immunofluorescence microscopy of cilia and flagella. *Methods Cell Biol.* 1995; 47:163–9. [https://doi.org/10.1016/s0091-679x\(08\)60805-5](https://doi.org/10.1016/s0091-679x(08)60805-5) PMID: 7476482
63. Jarvik JW, Rosenbaum JL. Oversized flagellar membrane protein in paralyzed mutants of *Chlamydomonas reinhardtii*. *J Cell Biol.* 1980; 85(2):258–72. <https://doi.org/10.1083/jcb.85.2.258> PMID: 7372708
64. Schneider CA, Rasband WS, Eliceiri KW. NIH Image to ImageJ: 25 years of image analysis. *Nat Methods.* 2012; 9(7):671–5. <https://doi.org/10.1038/nmeth.2089> PMID: 22930834
65. Yamamoto R, Yagi T, Kamiya R. Functional binding of inner-arm dyneins with demembrated flagella of *Chlamydomonas* mutants. *Cell Motil Cytoskeleton.* 2006; 63(5):258–65. <https://doi.org/10.1002/cm.20121> PMID: 16518818
66. Piperno G. Regulation of dynein activity within *Chlamydomonas* flagella. *Cell Motil Cytoskeleton.* 1995; 32(2):103–5. <https://doi.org/10.1002/cm.970320206> PMID: 8681388
67. Kagami O, Kamiya R. Translocation and rotation of microtubules caused by multiple species of *Chlamydomonas* inner-arm dynein. *J Cell Sci.* 1992; 103(3):653–64.
68. Sakakibara H, Takada S, King SM, Witman GB, Kamiya R. A *Chlamydomonas* outer arm dynein mutant with a truncated beta heavy chain. *J Cell Biol.* 1993; 122(3):653–61. <https://doi.org/10.1083/jcb.122.3.653> PMID: 8335691
69. Liu Z, Takazaki H, Nakazawa Y, Sakato M, Yagi T, Yasunaga T, et al. Partially functional outer-arm dynein in a novel *Chlamydomonas* mutant expressing a truncated gamma heavy chain. *Eukaryot Cell.* 2008; 7(7):1136–45. <https://doi.org/10.1128/EC.00102-08> PMID: 18487347
70. Myster SH, Knott JA, O'Toole E, Porter ME. The *Chlamydomonas* Dhc1 gene encodes a dynein heavy chain subunit required for assembly of the I1 inner arm complex. *Mol Biol Cell.* 1997; 8(4):607–20. <https://doi.org/10.1091/mbc.8.4.607> PMID: 9247642
71. Perrone CA, Myster SH, Bower R, O'Toole ET, Porter ME. Insights into the structural organization of the I1 inner arm dynein from a domain analysis of the 1beta dynein heavy chain. *Mol Biol Cell.* 2000; 11(7):2297–313. <https://doi.org/10.1091/mbc.11.7.2297> PMID: 10888669
72. Saitou N, Nei M. The neighbor-joining method: a new method for reconstructing phylogenetic trees. *Mol Biol Evol.* 1987; 4(4):406–25. <https://doi.org/10.1093/oxfordjournals.molbev.a040454> PMID: 3447015
73. Felsenstein J. Confidence limits on phylogenies: an approach using the bootstrap. *Evolution.* 1985; 39(4):783–91. <https://doi.org/10.1111/j.1558-5646.1985.tb00420.x> PMID: 28561359
74. Nei M, Kumar S. *Molecular Evolution and Phylogenetics*: Oxford University Press, New York; 2000.